

000 001 002 003 004 005 ALPHA DRIVE: UNLEASHING THE POWER OF VLMs IN 006 AUTONOMOUS DRIVING VIA RL AND REASONING 007 008 009

010 **Anonymous authors**
011 Paper under double-blind review
012
013
014
015
016
017
018
019
020
021
022
023
024
025
026
027
028

ABSTRACT

029
030 OpenAI o1 and DeepSeek R1 achieve or even surpass human expert-level per-
031 formance in complex domains like mathematics and science, with reinforcement
032 learning (RL) and reasoning playing a crucial role. In autonomous driving, recent
033 data-driven end-to-end models have greatly improved planning performance but
034 still struggle with long-tailed problems due to the inherent data imbalance. Some
035 studies integrate vision-language models (VLMs) into autonomous driving, but
036 they typically rely on pre-trained models with simple supervised fine-tuning (SFT)
037 on driving data, without further exploration of training strategies or optimizations
038 specifically tailored for planning. In this paper, we propose AlphaDrive, a RL and
039 reasoning framework for VLMs in autonomous driving. AlphaDrive introduces
040 four planning-oriented RL rewards based on Group Relative Policy Optimization
041 (GRPO) and employs a two-stage planning reasoning training strategy that com-
042 bines SFT with RL. As a result, AlphaDrive significantly improves both planning
043 performance and training efficiency compared to using only SFT or without rea-
044 soning. Moreover, we are also excited to discover that, following RL training,
045 AlphaDrive exhibits some emergent multimodal planning capabilities, which is
046 critical for improving driving safety and efficiency. To the best of our knowledge,
047 AlphaDrive is the first to integrate GRPO-based RL with VLMs in the context of
048 autonomous driving. Code will be released to facilitate future research.
049

1 INTRODUCTION

050 Autonomous driving has witnessed rapid advances in recent years, with end-to-end autonomous
051 driving emerging as one of the most representative models (Hu et al., 2023; Jiang et al., 2023; Chen
052 et al., 2024a; Prakash et al., 2021; Liao et al., 2024). They take sensor data as input and leverage
053 learnable neural networks to plan the vehicle’s future trajectory. Benefiting from large-scale driving
054 demonstrations, end-to-end models continuously improving their planning capabilities by expanding
055 training data and increasing model parameters.

056 However, due to their black-box nature and lack of common sense, end-to-end models still face
057 significant challenges when handling complex and long-tail driving scenarios. For instance, consider
058 a situation where the vehicle ahead is carrying traffic cones while driving. An end-to-end model may
059 fail to comprehend the relationship between the leading vehicle and the traffic cones, mistakenly
060 assuming that the road ahead is under construction and thus impassable, leading to an incorrect
061 decision to brake. Therefore, relying solely on end-to-end models to achieve high-level autonomous
062 driving remains challenging.

063 With the success of GPT (Brown et al., 2020), large language models (LLMs) show remarkable
064 comprehension and reasoning abilities (Touvron et al., 2023; Yang et al., 2024). Furthermore,
065 their capabilities have evolved from unimodal text understanding to multimodal vision-language
066 processing. (Liu et al., 2024; Chen et al., 2024c; Bai et al., 2023). The pre-trained knowledge and
067 reasoning abilities of VLMs hold great potential to mitigate the limitations of end-to-end models.

068 Recently, OpenAI’s o1 and o3 (OpenAI, 2024), which incorporate reasoning techniques, achieve
069 performance comparable to or even surpassing that of human experts in fields such as programming.
070 Additionally, DeepSeek R1 (Guo et al., 2025), which leverages reinforcement learning, not only
071 demonstrates “emergent capabilities” and achieves top-tier performance but also requires significantly
072

lower training costs compared to other models. These advances underscore the immense potential of reasoning techniques and RL in the development of large models.

Existing research on applying VLMs to autonomous driving can be broadly categorized into two directions. The first focuses on leveraging VLMs for the understanding of driving scenes (Sima et al., 2023; Zhou et al., 2024). The second explores the use of VLMs for planning, where some studies treat VLMs as end-to-end systems that process driving images and other inputs to directly predict trajectories (Xu et al., 2023; Chen et al., 2023). However, unlike end-to-end models which are specifically designed for trajectory planning, VLMs operate in a language space and are not inherently suited for precise numerical predictions (Frieder et al., 2024). Consequently, directly employing VLMs for trajectory planning may result in suboptimal performance and even pose safety risks.

Some studies leverage VLMs for high-level planning by formulating the ego vehicle’s future actions in natural language, such as “slow down and turn right” (Jiang et al., 2024). Although this approach circumvents the aforementioned drawbacks, existing works still lack further exploration of training methodologies. Most of them primarily rely on SFT, overlooking the impact of different training strategies on planning performance and the associated training costs.

In this paper, we explore the following question: How can RL and reasoning techniques of VLMs, which have achieved remarkable success in general domains, be applied to autonomous driving to improve planning performance while reducing training costs?

Through preliminary experiments, we find that directly applying existing RL and reasoning techniques to planning results in suboptimal performance. We attribute this to three main factors. First, the reward design in RL for general tasks is not well-suited for planning. For example, in visual object counting, the reward can be simply determined based on whether the model predicts the correct answer. However, in autonomous driving, while high-level planning can be formulated as a multi-class classification problem, the varying significance of different driving behaviors makes it inappropriate to assign equal weights to all actions.

Second, unlike mathematical or counting, the solution of planning are usually not unique. For instance, on an open, straight road, one may choose to maintain a constant speed or accelerate, both of which are valid decisions. Therefore, rigidly assessing whether the model’s planning output exactly matches the ground truth in the training data may not be the optimal approach.

Finally, while domains such as mathematics have abundant reasoning data, such as textbooks and solution manuals, autonomous driving lacks readily available datasets that capture the reasoning process. Collecting such data is highly costly and requires extensive manual annotation. As a result, directly applying existing reasoning techniques to planning remains challenging.

To address the aforementioned challenges, this paper introduces AlphaDrive, a VLM-based reinforcement learning and reasoning framework specifically designed for autonomous driving planning. In particular, AlphaDrive employs a RL strategy based on Group Relative Policy Optimization (GRPO) (Shao et al., 2024). Compared to Proximal Policy Optimization (PPO) (Schulman et al., 2017) and Direct Preference Optimization (DPO) (Rafailov et al., 2023), GRPO exhibits better training stability and performance. Furthermore, the group relative optimization strategy is well-suited for planning, as planning often involves multiple valid solutions, making relative optimization across multiple solutions a natural fit. Our experiments show that AlphaDrive exhibits some emergent multimodal planning capabilities, which we think can be attributed to the use of GRPO.

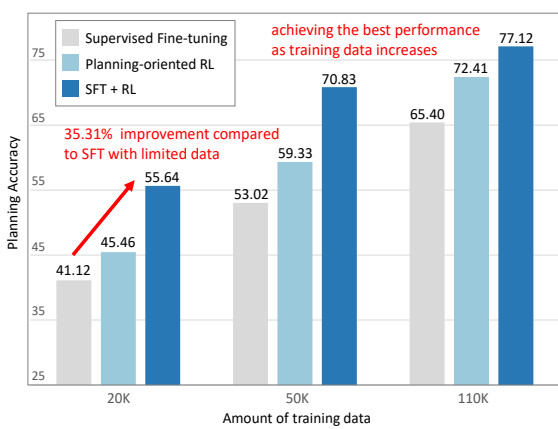


Figure 1: Our planning-oriented RL and two-stage training strategy significantly boost planning accuracy. With limited training data (only 20k samples), it greatly outperforms SFT by 35.31%. As training data increase, AlphaDrive consistently leads in planning performance.

108 AlphaDrive introduces four GRPO rewards tailored for planning. The first is the planning accuracy
 109 reward, which evaluates the consistency between the model’s planning actions and the ground truth
 110 actions. The second is the action-weighted reward, which assigns different weights to various actions
 111 based on their importance to safety. For instance, actions such as braking and steering are critical for
 112 safety, so weighting them accordingly helps the model achieve better performance in planning key
 113 actions. The third is the planning diversity reward, which encourages the model to generate multiple
 114 diverse solutions. This prevents mode collapse and enhances overall planning performance. The last
 115 one is the planning format reward, where we define a specific output format and encourage the model
 116 to follow it. This ensures more structured outputs and contributes to more stable training.

117 In addition to RL, we propose a planning reasoning technique which employs a two-stage training
 118 strategy based on knowledge distillation, integrating SFT and RL. In the first stage, we leverage a
 119 large cloud-based VLM to generate a small yet high-quality dataset, containing planning reasoning
 120 processes derived from real driving actions. This dataset is then used to fine-tune our model via
 121 SFT, effectively distilling knowledge from the large model. In the second stage, we further refine
 122 the model using RL. Introducing SFT as a warm-up stage effectively mitigates hallucinations and
 123 instability commonly observed in the early stages of RL, while also enhancing planning performance.

124 Our contributions are summarized as follows:

- 126 • We propose AlphaDrive, a VLM tailored for high-level planning in autonomous driving. To the
 127 best of our knowledge, AlphaDrive is the first to integrate GRPO-based RL with VLMs in the
 128 context of autonomous driving, significantly boosting both performance and training efficiency.
- 129 • AlphaDrive introduces four planning-oriented GRPO rewards: planning accuracy reward, action-
 130 weighted reward, planning diversity reward, and planning format reward. These optimized rewards
 131 make GRPO more suitable for autonomous driving.
- 132 • We propose a two-stage reasoning training strategy based on knowledge distillation, integrating
 133 SFT and RL. Our approach achieves better planning performance compared to training with RL
 134 alone or without reasoning.
- 135 • Extensive experiments and ablations on two datasets validate the superiority of AlphaDrive.
 136 Compared to the SFT-trained model, AlphaDrive significantly improves the planning accuracy by
 137 25.52% and, with only 20% of the training data, outperforms the SFT-trained model by 35.31%.
 138 We are also excited to discover that, following RL training, AlphaDrive exhibits some emergent
 139 multimodal planning capabilities, which is promising for improving driving safety and efficiency.

141 2 RELATED WORK

143 **Vision Language Models.** The capabilities of large models have greatly expanded from single
 144 modality to multi-modalities recently (Brown et al., 2020). Large VLMs (Achiam et al., 2023;
 145 Chen et al., 2024b) now demonstrate superior abilities in visual understanding and reasoning.
 146 Early works (Alayrac et al., 2022; Li et al., 2022; 2023) attempt to integrate visual models with
 147 large language models (LLMs) through attention mechanism and cross-modal contrastive learning.
 148 LLaVA (Liu et al., 2024) proposes using vanilla MLP as the connector between the visual encoder
 149 and LLMs, which achieves impressive visual understanding capabilities with relatively limited data.
 150 The QwenVL series (Bai et al., 2023; Wang et al., 2024a) continuously improve the visual module,
 151 offering better support for high-resolution and dynamic resolution images, while also demonstrate
 152 excellent performance in multilingual tasks and spatial perception.

153 **Reinforcement Learning and Reasoning.** Besides auto-regressive pretraining (Radford et al., 2018),
 154 RL and reasoning techniques further enhance the capabilities of large models (Schulman et al., 2017;
 155 Wei et al., 2022). For instance, GPT (Achiam et al., 2023) employs RL with Human Feedback
 156 (RLHF) (Ouyang et al., 2022), incorporating human preferences into training. By integrating human
 157 behavioral preferences, RLHF enables LLMs to generate outputs that align more closely with human
 158 preferences. Direct Preference Optimization (DPO) (Rafailov et al., 2023) enhances the model’s
 159 performance by directly optimizing preference feedback. Building on this, Group Relative Policy
 160 Optimization (GRPO) (Shao et al., 2024) introduces group relative optimization, which considers the
 161 relative advantages between multiple outputs, further improving training stability and effectiveness.
 The recent DeepSeek R1 (Guo et al., 2025) experiences an “Aha Moment” during training based on

162 GRPO, where, without any explicit guidance, the model autonomously allocates more thinking to
 163 the problem and re-evaluates its initial approach. This highlights the potential of RL in enabling
 164 large models to evolve from mere imitation to emergent intelligence. In our experiments, we are also
 165 excited to discover that, after GRPO-based RL training, AlphaDrive demonstrates some emergent
 166 multimodal planning capabilities, enabling it to generate multiple reasonable driving plans. We
 167 believe it has great potential to improve driving safety and efficiency.

168 In terms of reasoning, Chain-of-thought (Wei et al., 2022) has demonstrated great performance in
 169 solving complex problems by breaking them down and reasoning step by step. OpenAI o1 (OpenAI,
 170 2024), which is based on Chain-of-thought, introduces inference-time scaling. By increasing the
 171 computational cost during inference and combining search strategies such as Monte Carlo Tree Search
 172 (MCTS) (Świechowski et al., 2023) and Beam Search (Xie et al., 2023), significant improvements
 173 have been achieved in areas such as science and programming that require complex reasoning. This
 174 also shows that, beyond scaling model parameters and training data, scaling the inference-time
 175 computation is also a promising direction for exploration.

176 **Autonomous Driving Planning.** Planning is the ultimate task of autonomous driving. The earliest
 177 planning algorithms are rule-based (Paden et al., 2016; Thrun et al., 2006), which have significant
 178 limitations in terms of generalizability and efficiency. Recently, end-to-end models (Hu et al., 2023;
 179 Jiang et al., 2023; Chen et al., 2024a; Prakash et al., 2021; Liao et al., 2024; Gao et al., 2025) has
 180 gained popularity, where a unified neural network is used to directly output planning trajectories
 181 or control signals from sensor data. By leveraging large-scale driving demonstrations, end-to-end
 182 models are trained in a data-driven manner, achieving impressive planning performance. However,
 183 since end-to-end models are black-box models that lack common-sense and reasoning capabilities,
 184 they still struggle to address the long-tailed problems in autonomous driving.

185 **VLMs and Autonomous Driving.** The common-sense and reasoning capabilities of large models can
 186 effectively compensate the limitations of end-to-end models. DriveGPT4 (Xu et al., 2023) employs a
 187 VLM that takes front-view videos as input and directly predicts control signals. ELM (Zhou et al.,
 188 2024) trains on large-scale, cross-domain video data, showing that diverse data sources can improve
 189 VLM performance on driving tasks. OmniDrive (Wang et al., 2024b) introduces sparse 3D tokens to
 190 represent driving scenes, which are then input into VLMs for scene understanding and planning.

191 In addition to the above works that directly apply VLMs for driving, DriveVLM (Tian et al., 2024)
 192 combines VLMs with end-to-end models, where VLMs predict low-frequency waypoints and end-to-
 193 end models generate high-frequency trajectories. Senna (Jiang et al., 2024) proposes to use VLMs for
 194 high-level planning and end-to-end models for low-level trajectory prediction. Several datasets and
 195 benchmarks (Sima et al., 2023; Qian et al., 2024) have also been introduced to advance VLM use in
 196 autonomous driving. However, most existing work relies on pre-trained models followed by SFT on
 197 driving data, lacking exploration of training strategies tailored to planning. Further effort is needed to
 198 adapt the impressive RL and reasoning techniques from general tasks to autonomous driving.

200 3 ALPHADRIVE 201

202 AlphaDrive is a VLM designed for autonomous driving planning. Unlike previous approaches that
 203 rely solely on SFT, we explore the incorporation of RL and reasoning techniques to better align
 204 with the unique characteristics of driving planning: (1) the varying importance of different driving
 205 behaviors; (2) the existence of multiple feasible solutions; and (3) the scarcity of readily available
 206 reasoning data for planning decisions.

207 We propose four GRPO-based RL rewards tailored for planning, along with a two-stage training
 208 strategy that integrates SFT with RL. Our experiments demonstrate that, compared to using SFT
 209 alone or training without reasoning, AlphaDrive achieves significant improvements in both planning
 210 performance and training efficiency. In the following, we will detail the design of each component.

212 3.1 PLANNING-ORIENTED REINFORCEMENT LEARNING 213

214 Current commonly used RL algorithms include PPO (Schulman et al., 2017), DPO (Rafailov et al.,
 215 2023), and GRPO (Shao et al., 2024). We ultimately choose GRPO for two key reasons: DeepSeek
 R1 (Guo et al., 2025) has demonstrated the effectiveness of GRPO in general domains. Compared to

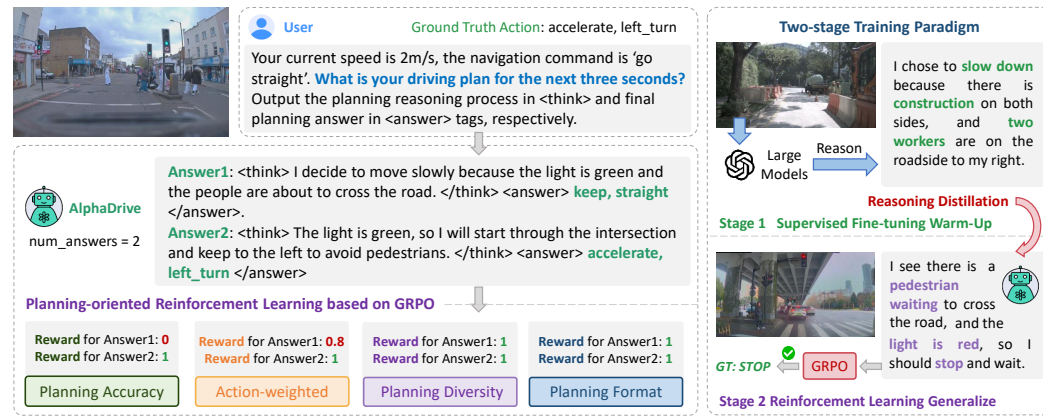


Figure 2: **Overall framework of AlphaDrive.** AlphaDrive is trained using GRPO-based RL, and we design four planning rewards to help the model understand and learn planning. Besides, we propose a two-stage training paradigm, the first stage uses SFT to distill the planning reasoning process from a large model and serves as a warm-up, while the second stage employs RL to explore planning.

other algorithms, GRPO provides higher training stability and efficiency. Moreover, the group relative optimization strategy introduced by GRPO is particularly well-suited for planning, as planning often involves multiple valid solutions, making relative optimization across multiple solutions is a natural fit. Experimental results further confirm that models trained with GRPO exhibit strong planning capabilities.

Given a query q , GRPO samples a group of outputs $\{o_1, o_2, \dots, o_G\}$ from the old policy $\pi_{\theta_{old}}$ and optimizes the new policy π_{θ} by maximizing:

$$\mathcal{J}_{\text{GRPO}}(\theta) = \mathbb{E}_{q, \{o_i\} \sim \pi_{\theta_{old}}} \left[\frac{1}{G} \sum_{i=1}^G \mathcal{L}_i - \beta \mathbb{D}_{KL}(\pi_{\theta} \parallel \pi_{ref}) \right], \quad (1)$$

$$\mathcal{L}_i = \min(w_i A_i, \text{clip}(w_i, 1 - \epsilon, 1 + \epsilon) A_i), \quad (2)$$

where $w_i = \frac{\pi_{\theta}(o_i|q)}{\pi_{\theta_{old}}(o_i|q)}$, ϵ and β are hyper-parameters, and the advantage A_i is computed using the normalized reward within the group.

3.1.1 PLANNING REWARD MODELING

Planning Accuracy Reward. In fields such as mathematics or programming, the reward in GRPO can be intuitively determined based on whether the final answer is correct. However, planning is more complex, as it involves both lateral (direction) and longitudinal (speed) components. Furthermore, the set of possible actions is constrained. As a result, we use the F1-Score to evaluate the accuracy of both lateral and longitudinal decisions separately, and assign rewards accordingly.

Initially, we evaluate accuracy by checking whether the model’s prediction exactly matches the ground truth. However, due to imperfect format in the model’s early training phase, such as discrepancies in case sensitivity or the presence of extraneous outputs, this approach results in poor stability during the early stages of training. We then attempt to extract all the words from the prediction and check whether the ground truth is included among the words. This introduces a new issue where the model sometimes learns shortcut solutions, such as outputting all possible actions, which causes mode collapse. Ultimately, we adopt the F1-score for evaluation, as it not only prevents the model from learning shortcut solutions (where outputting all decisions could result in high recall but low accuracy) but also improves the stability during the early training phase.

Action-Weighted Reward. As mentioned above, the importance of different behaviors in planning varies. For instance, decelerating and stopping are more critical for safety than maintaining speed. Therefore, we assign different importance weights to various actions, incorporating them as weighted components in the final reward.

270

Algorithm 1: Planning Reward Modeling.

271

Input: Planning answers \mathcal{A} , Ground Truth action e , Action Weights \mathcal{W} , Planning Diversity Weight θ

272

Output: Planning Reward \mathcal{R}

273

1 Initialization: Planning Reward $\mathcal{R} \leftarrow \emptyset$, Speed Action Set \mathcal{S} , Path Action Set \mathcal{P} , Answer Format \mathcal{F}

274

2 # Pytorch-like Code

275

3 speed_cnt, path_cnt = Counter(), Counter()

276

4 **for** ans in \mathcal{A} **do**

277

5 action_ans = re.search(r“ \mathcal{F} ”, ans).group(1).strip()

278

6 speed_ans, path_ans = **extract_ans**(action_ans, \mathcal{S}), **extract_ans**(action_ans, \mathcal{P})

279

7 speed_cnt.update(speed_ans), path_cnt.update(path_cnt)

280

8 # Calculate Planning Accuracy Reward

281

9 speed_acc_R, path_acc_R = **cal_f1_score**(speed_ans, e), **cal_f1_score**(path_ans, e)

282

10 # Calculate Action-Weighted Reward

283

11 speed_weighted_R, path_weighted_R = \mathcal{W} [speed_ans], \mathcal{W} [path_ans]

284

12 # Calculate Planning Diversity Reward

285

13 speed_div_R, path_div_R = θ **if** speed_cnt[speed_ans] == 1 **else** $-\theta$, θ **if** path_cnt[path_ans] == 1 **else** $-\theta$

286

14 # Calculate Planning Format Reward

287

15 format_R = **check_format**(ans , \mathcal{F})

288

16 # Final Planning Quality Reward

289

17 speed_R = speed_acc_R * speed_weighted_R + speed_div_R

290

18 path_R = path_acc_R * path_weighted_R + path_div_R

291

19 \mathcal{R} .append([speed_R, path_R, format_R])

292

extrat_ans will extract substrings that match the specified pattern from the given string. **cal_f1_score** will calculate F1 score given the predictions and ground truth. **check_format** will check whether the given string matches the provided pattern based on regular expression matching.

293

294

Planning Diversity Reward. Since planning is inherently multimodal, during GRPO-based RL training, the model generates multiple solutions for group relative optimization. In the later stages of training, we observe that the model’s outputs tend to converge to the same solution. Our goal is to encourage the model to generate a variety of feasible solutions, rather than merely aligning with the ground truth actions in the training data. To achieve this, we propose the Planning Diversity Reward. When the model’s outputs differ, we assign a higher reward; otherwise, we reduce the reward.

301

Planning Format Reward. The last reward is used to regularize the output, making it easier to extract both the reasoning process and the final answer. This approach is inspired by R1. The reasoning process is encapsulated within the \langle think \rangle \langle /think \rangle tags, while the planning result is enclosed within the \langle answer \rangle \langle /answer \rangle tags. If the final output does not conform to this format, the format reward will be set to 0.

306

The Planning Accuracy Reward, the Action-Weighted Reward, and the Planning Diversity Reward are combined to compute the Planning Quality Reward. We calculate the Planning Quality Reward separately for speed planning and direction planning. Finally, the Planning Quality Reward and the Planning Format Reward are used to calculate the GRPO loss and update the model parameters. For details about Planning Reward Modeling, please refer to Alg. 1.

311

3.2 REASONING: DISTILLATION FROM LARGE MODELS

313

314

Unlike fields such as mathematics or science, which have abundant high-quality reasoning data available for training, the planning process in autonomous driving is difficult to record, and the cost of manual annotation is high. As a result, there is currently no large-scale, readily available planning reasoning dataset. We initially attempt to incorporate reasoning steps directly into the RL training process, but the final results are suboptimal, mainly due to the following shortcomings: (1) insufficient perception of key elements, such as traffic lights; (2) disorganized reasoning process with weak causal relationships; (3) reasoning outputs that are overly lengthy and ineffective.

315

316

317

318

319

320

321

322

323

Therefore, we adopt a more capable cloud-based large model Qwen2VL-72B, to generate high-quality planning reasoning data from a small set of driving clips. Specifically, we provide the model with prompts that include the real driving actions in a given scenario, along with the vehicle’s current state and navigation information, prompting the model to generate a concise decision-making process. We

324 Table 1: High-level planning and reasoning results on the MetaAD validation set. Except for
 325 AlphaDrive, which utilizes our proposed training strategy, all other models (Chen et al., 2024b; Wang
 326 et al., 2024a; Dubey et al., 2024) are fine-tuned with SFT on the MetaAD training set.
 327

328 Method	Train. Strategy	Acc. (%)	Path (F1) ↑			Speed (F1) ↑			BLEU-4	CIDEr	METEOR
			straight	left	right	keep	acc.	dec.			
InternVL2-2B	SFT	51.07	76.13	85.16	64.60	74.77	21.88	47.66	75.81	27.89	19.73
Qwen2VL-2B	SFT	55.84	82.68	80.31	70.04	75.97	34.92	55.55	72.64	24.46	23.14
Llama3.2-V-11B	SFT	58.21	85.58	84.64	79.12	74.79	35.56	58.99	76.20	32.05	21.25
Qwen2VL-7B	SFT	61.44	86.45	85.84	87.75	84.53	43.81	56.30	73.80	41.09	30.65
AlphaDrive-2B	Ours	77.12	96.62	89.83	93.25	86.80	56.33	71.40	86.63	43.54	38.97

334 Table 2: End-to-end planning results on the NAVSIM `navtest` split with closed-loop metrics. *
 335 denotes incorporating (Liao et al., 2024) as the end-to-end trajectory planning module.
 336

337 Method	338 Reference	339 NC ↑	340 DAC ↑	341 TTC ↑	342 Comf ↑	343 EP ↑	344 PDMS ↑
UniAD (Hu et al., 2023)	CVPR 23	97.8	91.9	92.9	100	78.8	83.4
PARA-Drive (Weng et al., 2024)	CVPR 24	97.9	92.4	93.0	99.8	79.3	84.0
Transfuser (Prakash et al., 2021)	PAMI 23	97.7	92.8	92.8	100	79.2	84.0
DRAMA (Yuan et al., 2024)	arXiv 23	98.0	93.1	94.8	100	80.1	85.5
VADV2 (Chen et al., 2024a)	arXiv 24	97.2	89.1	91.6	100	76.0	80.9
Hydra-MDP (Li et al., 2024)	arXiv 24	98.3	96.0	94.6	100	78.7	86.5
DiffusionDrive (Liao et al., 2024)	CVPR 25	98.2	96.2	94.7	100	82.2	88.1
AlphaDrive-SFT*	Baseline	98.1	96.4	95.0	100	82.4	88.3
AlphaDrive*	Ours	98.3	97.6	95.4	100	83.1	89.5

347 find that the quality of the generated reasoning process is overall satisfactory. After conducting a
 348 manual quality check and filtering out samples with obvious errors, we obtain a batch of high-quality
 349 planning reasoning data. Subsequently, our model can improve its planning reasoning ability through
 350 knowledge distillation based on this data.
 351

352 3.3 TRAINING: SFT WARM-UP, RL EXPLORATION

354 RL relies on sparse reward signals, whereas SFT is based on dense supervision, making it more
 355 suitable for knowledge distillation. Additionally, we find that relying solely on RL can lead to
 356 instability in the early stages of training. Therefore, we use a small amount of data for a warm-up
 357 phase based on SFT, followed by RL training with the full dataset. We discover that this approach
 358 improves stability in the early stages of training and enhances the model’s planning reasoning
 359 performance, ultimately leading to better overall planning capabilities.
 360

361 4 EXPERIMENTS

363 **Dataset.** We adopt two datasets, MetaAD and NAVSIM (Dauner et al., 2024). MetaAD is a large-
 364 scale real-world driving dataset which consists of 120k driving clips, each lasting three seconds.
 365 It supports multi-sensor data and perception annotations, as well as maintaining a well-balanced
 366 distribution across various driving scenarios and planning actions. The dataset is divided into 110k
 367 clips for training and 10k clips for validation. As for reasoning, we sample 30k data from the training
 368 dataset to generate the planning reasoning data. We conduct ablations on the MetaAD dataset by
 369 default.
 370

NAVSIM (Dauner et al., 2024) is a widely used planning benchmark that includes surround-view
 371 images from eight cameras, LiDAR point clouds, high-definition maps, and object detection annota-
 372 tions. The dataset supports non-reactive simulations and provides closed-loop evaluation metrics,
 373 allowing for comprehensive evaluation of autonomous planning methods. More information about
 374 the dataset and ablations can be found in Appendix A due to page limit.
 375

Training Details. We use Qwen2VL-2B (Wang et al., 2024a) as the base model. Qwen2VL is
 376 currently one of the best-performing open-source models, and it offers a smaller 2B version that better
 377 meets the latency requirements for autonomous driving. The model’s inputs include a front-view
 378 image and a planning prompt, which contains the vehicle’s current speed and navigation information.
 379

Table 3: Ablations on the effectiveness of our proposed planning GRPO rewards.

Table 4: Ablations on different reasoning training strategies.

The navigation data, consistent with real-world driving, is obtained from sparse navigation points via AMap (similar to Google Maps) and is converted into text form for inclusion in the prompt, such as “Go straight for 100m, then turn right”. The training settings follows Qwen2VL, and all experiments are conducted using 16 NVIDIA A800 GPUs.

Evaluation. For high-level planning, the evaluation metrics consist of two aspects. First, the accuracy of meta-action planning is measured by calculating the F1-Score for all categories of lateral and longitudinal meta-actions, followed by the overall planning accuracy. Additionally, for planning reasoning, we compute the similarity between the generated planning reasoning process and the annotated reasoning process in the dataset using BLEU-4 (Papineni et al., 2002), CIDEr (Vedantam et al., 2015), and METEOR (Banerjee & Lavie, 2005) scores. In terms of end-to-end planning, we adopt the closed-loop metrics such as PDMS proposed in NAVSIM for evaluation.

LLM Usage. We used existing LLMs/VLMs in two ways. As described in Sec. 3.2, Qwen2VL-72B was employed to generate planning-reasoning text for the SFT training data. Additionally, GPT-5 was used for language polishing. The authors take full responsibility for all generated content.

4.1 MAIN RESULTS

High-level Planning. Tab. 1 presents the performance of AlphaDrive in high-level planning. As shown, AlphaDrive significantly outperforms the other models. Compared to Qwen2VL-7B, the second-best performing model after AlphaDrive, the planning accuracy significantly improves by 25.5%. There is a noticeable enhancement in key decisions such as steering and acceleration/deceleration. Additionally, the quality of planning reasoning is the best among all models, demonstrating the effectiveness of our proposed two-stage RL training and reasoning strategies.

End-to-end Trajectory Planning. Besides high-level planning, we further integrate AlphaDrive with an existing end-to-end model to evaluate its contribution to trajectory planning. Specifically, AlphaDrive is first trained on NAVSIM using the same pipeline as the MetaAD dataset. Its high-level decisions are then mapped to high-dimensional features via learnable embeddings and fed as conditional inputs to the DiffusionDrive decoder to generate the final trajectory. As shown in Table 2, the SFT-trained baseline achieves only a marginal improvement, while AlphaDrive, trained with our proposed strategy, achieves the best planning performance, with a PDMS score of 89.5.

4.2 ABLATION STUDY

Planning Rewards. In Tab. 3, we validate the effectiveness of the proposed planning GRPO rewards. Base Accuracy Reward directly determines the reward based on whether the response exactly matches

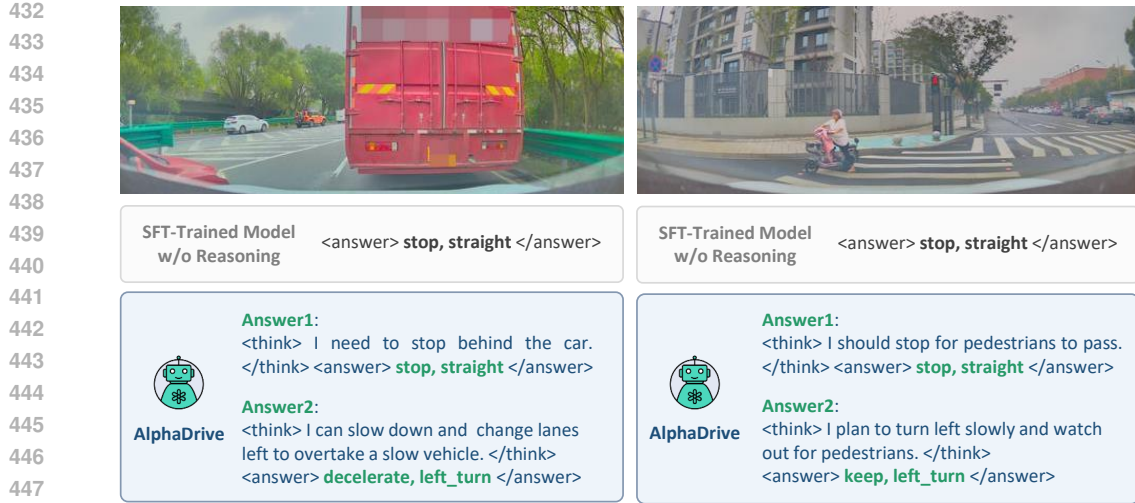


Figure 3: Qualitative results of AlphaDirve. After RL training, AlphaDrive exhibits some emergent multimodal planning capabilities, which has great potential for improving planning performance.

452 the ground truth, a common approach in general domains. As shown, the model using the Base
453 Accuracy reward lags significantly behind across all metrics (ID 1). The combination with the
454 Planning Format Reward yields a slight improvement. (ID 2). A significant improvement is seen
455 with the adoption of our proposed Planning Accuracy Reward (ID 3). Further enhancement in
456 acceleration/deceleration is achieved by incorporating the Action-Weighted Reward (ID 4). Finally,
457 by combining the Planning Diversity Reward, the best planning performance is achieved (ID 5-6).

458 **Reasoning Training Strategies.** The ablations of the reasoning training strategies is shown in
459 Tab. 4. Introducing planning reasoning under various training strategies effectively enhances model
460 performance, particularly for complex actions like acceleration and deceleration. This highlights
461 reasoning’s impact on decision-making in challenging scenarios. Notably, the RL-trained-only model
462 underperforms in reasoning compared to the SFT-trained one, which we attribute to the limited model
463 size that constrains its perception and reasoning capabilities. Incorporating SFT as a warm-up and
464 using knowledge distillation to learn the reasoning process from a larger model helps mitigate this.
465 Combining SFT and RL yields the best planning reasoning capabilities.

466 467 4.3 EMERGENCE OF MULTIMODAL PLANNING CAPABILITY

468 Fig. 3 illustrates the multimodal planning capability of AlphaDrive after RL training. In complex
469 scenarios, it can effectively generate multiple feasible solutions. Although SFT-trained model can
470 also generate multiple answers through sampling, its multimodal planning capability remains limited,
471 as shown in our ablation study (Tab. 6). AlphaDrive can be integrated with a downstream action
472 model to dynamically select the optimal solution from multiple options.

474 5 CONCLUSIONS AND LIMITATIONS

475 In this work, we propose AlphaDrive, a VLM for high-level planning in autonomous driving.
476 Compared to previous models that solely employed the SFT, we explore the integration of advanced
477 RL and reasoning in planning. Specifically, AlphaDrive introduces a planning-oriented RL strategy
478 based on GRPO and further designs a two-stage planning reasoning training paradigm. To the best of
479 our knowledge, AlphaDrive is the first to integrate GRPO-based RL with VLMs in the context of
480 autonomous driving, significantly boosting both performance and training efficiency.

481 Currently, due to a lack of rich data annotation, AlphaDrive is still unable to output more complex
482 driving behaviors such as lane changes or nudges. Additionally, the current planning reasoning data
483 come from pseudo-labels generated by large models based on ground-truth driving actions, which still
484 suffer from inaccurate perception and a failure to capture key factors. Therefore, further systematic
485 validation is required to improve data quality and verify the performance upper bound.

486 REFERENCES
487

488 Josh Achiam, Steven Adler, Sandhini Agarwal, Lama Ahmad, Ilge Akkaya, Florencia Leoni Aleman,
489 Diogo Almeida, Janko Altenschmidt, Sam Altman, Shyamal Anadkat, et al. Gpt-4 technical report.
490 *arXiv preprint arXiv:2303.08774*, 2023.

491 Jean-Baptiste Alayrac, Jeff Donahue, Pauline Luc, Antoine Miech, Iain Barr, Yana Hasson, Karel
492 Lenc, Arthur Mensch, Katherine Millican, Malcolm Reynolds, et al. Flamingo: a visual language
493 model for few-shot learning. *Advances in neural information processing systems*, 2022.

494 Jinze Bai, Shuai Bai, Shusheng Yang, Shijie Wang, Sinan Tan, Peng Wang, Junyang Lin, Chang
495 Zhou, and Jingren Zhou. Qwen-vl: A frontier large vision-language model with versatile abilities.
496 *arXiv preprint arXiv:2308.12966*, 2023.

497 Satanjeev Banerjee and Alon Lavie. Meteor: An automatic metric for mt evaluation with improved
498 correlation with human judgments. In *Proceedings of the acl workshop on intrinsic and extrinsic*
499 *evaluation measures for machine translation and/or summarization*, 2005.

500 Tom Brown, Benjamin Mann, Nick Ryder, Melanie Subbiah, Jared D Kaplan, Prafulla Dhariwal,
501 Arvind Neelakantan, Pranav Shyam, Girish Sastry, Amanda Askell, et al. Language models are
502 few-shot learners. In *NeurIPS*, 2020.

503 Long Chen, Oleg Sinavski, Jan Hünermann, Alice Karnsund, Andrew James Willmott, Danny Birch,
504 Daniel Maund, and Jamie Shotton. Driving with llms: Fusing object-level vector modality for
505 explainable autonomous driving. *arXiv preprint arXiv:2310.01957*, 2023.

506 Shaoyu Chen, Bo Jiang, Hao Gao, Bencheng Liao, Qing Xu, Qian Zhang, Chang Huang, Wenyu Liu,
507 and Xinggang Wang. Vadv2: End-to-end vectorized autonomous driving via probabilistic planning.
508 *arXiv preprint arXiv:2402.13243*, 2024a.

509 Zhe Chen, Weiyun Wang, Yue Cao, Yangzhou Liu, Zhangwei Gao, Erfei Cui, Jinguo Zhu, Shenglong
510 Ye, Hao Tian, Zhaoyang Liu, et al. Expanding performance boundaries of open-source multimodal
511 models with model, data, and test-time scaling. *arXiv preprint arXiv:2412.05271*, 2024b.

512 Zhe Chen, Jiannan Wu, Wenhai Wang, Weijie Su, Guo Chen, Sen Xing, Muyan Zhong, Qinglong
513 Zhang, Xizhou Zhu, Lewei Lu, et al. Internvl: Scaling up vision foundation models and aligning
514 for generic visual-linguistic tasks. In *CVPR*, 2024c.

515 Daniel Dauner, Marcel Hallgarten, Tianyu Li, Xinshuo Weng, Zhiyu Huang, Zetong Yang, Hongyang
516 Li, Igor Gilitschenski, Boris Ivanovic, Marco Pavone, et al. Navsim: Data-driven non-reactive
517 autonomous vehicle simulation and benchmarking. *NeurIPS*, 2024.

518 Alexey Dosovitskiy, Lucas Beyer, Alexander Kolesnikov, Dirk Weissenborn, Xiaohua Zhai, Thomas
519 Unterthiner, Mostafa Dehghani, Matthias Minderer, Georg Heigold, Sylvain Gelly, et al. An
520 image is worth 16x16 words: Transformers for image recognition at scale. *arXiv preprint*
521 *arXiv:2010.11929*, 2020.

522 Abhimanyu Dubey, Abhinav Jauhri, Abhinav Pandey, Abhishek Kadian, Ahmad Al-Dahle, Aiesha
523 Letman, Akhil Mathur, Alan Schelten, Amy Yang, Angela Fan, et al. The llama 3 herd of models.
524 *arXiv preprint arXiv:2407.21783*, 2024.

525 Simon Frieder, Luca Pinchetti, Ryan-Rhys Griffiths, Tommaso Salvatori, Thomas Lukasiewicz,
526 Philipp Petersen, and Julius Berner. Mathematical capabilities of chatgpt. In *NeurIPS*, 2024.

527 Hao Gao, Shaoyu Chen, Bo Jiang, Bencheng Liao, Yiang Shi, Xiaoyang Guo, Yuechuan Pu, Haoran
528 Yin, Xiangyu Li, Xinbang Zhang, et al. Rad: Training an end-to-end driving policy via large-scale
529 3dgs-based reinforcement learning. *arXiv preprint arXiv:2502.13144*, 2025.

530 Daya Guo, Dejian Yang, Huawei Zhang, Junxiao Song, Ruoyu Zhang, Runxin Xu, Qihao Zhu,
531 Shirong Ma, Peiyi Wang, Xiao Bi, et al. Deepseek-r1: Incentivizing reasoning capability in llms
532 via reinforcement learning. *arXiv preprint arXiv:2501.12948*, 2025.

533 Yihan Hu, Jiazhi Yang, Li Chen, Keyu Li, Chonghao Sima, Xizhou Zhu, Siqi Chai, Senyao Du,
534 Tianwei Lin, Wenhai Wang, et al. Planning-oriented autonomous driving. In *CVPR*, 2023.

540 Bo Jiang, Shaoyu Chen, Qing Xu, Bencheng Liao, Jiajie Chen, Helong Zhou, Qian Zhang, Wenyu Liu,
 541 Chang Huang, and Xinggang Wang. Vad: Vectorized scene representation for efficient autonomous
 542 driving. In *ICCV*, 2023.

543

544 Bo Jiang, Shaoyu Chen, Bencheng Liao, Xingyu Zhang, Wei Yin, Qian Zhang, Chang Huang,
 545 Wenyu Liu, and Xinggang Wang. Senna: Bridging large vision-language models and end-to-end
 546 autonomous driving. *arXiv preprint arXiv:2410.22313*, 2024.

547 Junnan Li, Dongxu Li, Caiming Xiong, and Steven Hoi. Blip: Bootstrapping language-image
 548 pre-training for unified vision-language understanding and generation. In *ICML*, 2022.

549

550 Junnan Li, Dongxu Li, Silvio Savarese, and Steven Hoi. Blip-2: Bootstrapping language-image
 551 pre-training with frozen image encoders and large language models. In *ICML*, 2023.

552 Zhenxin Li, Kailin Li, Shihao Wang, Shiyi Lan, Zhiding Yu, Yishen Ji, Zhiqi Li, Ziyue Zhu, Jan Kautz,
 553 Zuxuan Wu, et al. Hydra-mdp: End-to-end multimodal planning with multi-target hydra-distillation.
 554 *arXiv preprint arXiv:2406.06978*, 2024.

555

556 Bencheng Liao, Shaoyu Chen, Haoran Yin, Bo Jiang, Cheng Wang, Sixu Yan, Xinbang Zhang,
 557 Xiangyu Li, Ying Zhang, Qian Zhang, et al. Diffusiondrive: Truncated diffusion model for
 558 end-to-end autonomous driving. *arXiv preprint arXiv:2411.15139*, 2024.

559

560 Haotian Liu, Chunyuan Li, Qingyang Wu, and Yong Jae Lee. Visual instruction tuning. In *NeurIPS*,
 561 2024.

562 OpenAI. Learning to reason with llms, 2024. URL <https://openai.com/index/learning-to-reason-with-llms/>.

563

564 Long Ouyang, Jeffrey Wu, Xu Jiang, Diogo Almeida, Carroll Wainwright, Pamela Mishkin, Chong
 565 Zhang, Sandhini Agarwal, Katarina Slama, Alex Ray, et al. Training language models to follow
 566 instructions with human feedback. *Advances in neural information processing systems*, 2022.

567

568 Brian Paden, Michal Čáp, Sze Zheng Yong, Dmitry Yershov, and Emilio Frazzoli. A survey of motion
 569 planning and control techniques for self-driving urban vehicles. *IEEE Transactions on intelligent
 570 vehicles*, 2016.

571

572 Kishore Papineni, Salim Roukos, Todd Ward, and Wei-Jing Zhu. Bleu: a method for automatic
 573 evaluation of machine translation. In *ACL*, 2002.

574

575 Aditya Prakash, Kashyap Chitta, and Andreas Geiger. Multi-modal fusion transformer for end-to-end
 576 autonomous driving. In *CVPR*, 2021.

577

578 Tianwen Qian, Jingjing Chen, Linhai Zhuo, Yang Jiao, and Yu-Gang Jiang. Nuscenes-qa: A multi-
 579 modal visual question answering benchmark for autonomous driving scenario. In *AAAI*, 2024.

580

581 Alec Radford, Karthik Narasimhan, Tim Salimans, Ilya Sutskever, et al. Improving language
 582 understanding by generative pre-training. *OpenAI*, 2018.

583

584 Alec Radford, Jong Wook Kim, Chris Hallacy, Aditya Ramesh, Gabriel Goh, Sandhini Agarwal,
 585 Girish Sastry, Amanda Askell, Pamela Mishkin, Jack Clark, et al. Learning transferable visual
 586 models from natural language supervision. In *ICML*, 2021.

587

588 Rafael Rafailov, Archit Sharma, Eric Mitchell, Christopher D Manning, Stefano Ermon, and Chelsea
 589 Finn. Direct preference optimization: Your language model is secretly a reward model. *Advances
 590 in Neural Information Processing Systems*, 36:53728–53741, 2023.

591

592 John Schulman, Filip Wolski, Prafulla Dhariwal, Alec Radford, and Oleg Klimov. Proximal policy
 593 optimization algorithms. *arXiv preprint arXiv:1707.06347*, 2017.

594

595 Zhihong Shao, Peiyi Wang, Qihao Zhu, Runxin Xu, Junxiao Song, Xiao Bi, Haowei Zhang,
 596 Mingchuan Zhang, YK Li, Y Wu, et al. Deepseekmath: Pushing the limits of mathematical
 597 reasoning in open language models. *arXiv preprint arXiv:2402.03300*, 2024.

594 Chonghao Sima, Katrin Renz, Kashyap Chitta, Li Chen, Hanxue Zhang, Chengen Xie, Ping Luo,
 595 Andreas Geiger, and Hongyang Li. Drivelm: Driving with graph visual question answering. *arXiv*
 596 *preprint arXiv:2312.14150*, 2023.

597

598 Maciej Świechowski, Konrad Godlewski, Bartosz Sawicki, and Jacek Mańdziuk. Monte carlo tree
 599 search: A review of recent modifications and applications. *Artificial Intelligence Review*, 56(3):
 600 2497–2562, 2023.

601

602 Sebastian Thrun, Mike Montemerlo, Hendrik Dahlkamp, David Stavens, Andrei Aron, James Diebel,
 603 Philip Fong, John Gale, Morgan Halpenny, Gabriel Hoffmann, et al. Stanley: The robot that won
 604 the darpa grand challenge. *Journal of field Robotics*, 2006.

605

606 Xiaoyu Tian, Junru Gu, Bailin Li, Yicheng Liu, Chenxu Hu, Yang Wang, Kun Zhan, Peng Jia,
 607 Xianpeng Lang, and Hang Zhao. Drivevlm: The convergence of autonomous driving and large
 608 vision-language models. *arXiv preprint arXiv:2402.12289*, 2024.

609

610 Hugo Touvron, Thibaut Lavril, Gautier Izacard, Xavier Martinet, Marie-Anne Lachaux, Timothée
 611 Lacroix, Baptiste Rozière, Naman Goyal, Eric Hambro, Faisal Azhar, et al. Llama: Open and
 612 efficient foundation language models. *arXiv preprint arXiv:2302.13971*, 2023.

613

614 Ramakrishna Vedantam, C Lawrence Zitnick, and Devi Parikh. Cider: Consensus-based image
 615 description evaluation. In *CVPR*, 2015.

616

617 Peng Wang, Shuai Bai, Sinan Tan, Shijie Wang, Zhihao Fan, Jinze Bai, Keqin Chen, Xuejing Liu,
 618 Jialin Wang, Wenbin Ge, et al. Qwen2-vl: Enhancing vision-language model’s perception of the
 619 world at any resolution. *arXiv preprint arXiv:2409.12191*, 2024a.

620

621 Shihao Wang, Zhiding Yu, Xiaohui Jiang, Shiyi Lan, Min Shi, Nadine Chang, Jan Kautz, Ying Li,
 622 and Jose M Alvarez. Omnidrive: A holistic llm-agent framework for autonomous driving with 3d
 623 perception, reasoning and planning. *arXiv preprint arXiv:2405.01533*, 2024b.

624

625 Jason Wei, Xuezhi Wang, Dale Schuurmans, Maarten Bosma, Fei Xia, Ed Chi, Quoc V Le, Denny
 626 Zhou, et al. Chain-of-thought prompting elicits reasoning in large language models. *Advances in
 627 neural information processing systems*, 35:24824–24837, 2022.

628

629 Xinshuo Weng, Boris Ivanovic, Yan Wang, Yue Wang, and Marco Pavone. Para-drive: Parallelized
 630 architecture for real-time autonomous driving. In *CVPR*, 2024.

631

632 Yuxi Xie, Kenji Kawaguchi, Yiran Zhao, James Xu Zhao, Min-Yen Kan, Junxian He, and Michael
 633 Xie. Self-evaluation guided beam search for reasoning. *Advances in Neural Information Processing
 634 Systems*, 36:41618–41650, 2023.

635

636 Zhenhua Xu, Yujia Zhang, Enze Xie, Zhen Zhao, Yong Guo, Kenneth KY Wong, Zhenguo Li, and
 637 Hengshuang Zhao. Drivegpt4: Interpretable end-to-end autonomous driving via large language
 638 model. *arXiv preprint arXiv:2310.01412*, 2023.

639

640 An Yang, Baosong Yang, Binyuan Hui, Bo Zheng, Bowen Yu, Chang Zhou, Chengpeng Li,
 641 Chengyuan Li, Dayiheng Liu, Fei Huang, et al. Qwen2 technical report. *arXiv preprint
 642 arXiv:2407.10671*, 2024.

643

644 Chengran Yuan, Zhanqi Zhang, Jiawei Sun, Shuo Sun, Zefan Huang, Christina Dao Wen Lee, Dongen
 645 Li, Yuhang Han, Anthony Wong, Keng Peng Tee, et al. Drama: An efficient end-to-end motion
 646 planner for autonomous driving with mamba. *arXiv preprint arXiv:2408.03601*, 2024.

647

648 Yunsong Zhou, Linyan Huang, Qingwen Bu, Jia Zeng, Tianyu Li, Hang Qiu, Hongzi Zhu, Minyi
 649 Guo, Yu Qiao, and Hongyang Li. Embodied understanding of driving scenarios. *arXiv preprint
 650 arXiv:2403.04593*, 2024.

648 Table 5: High-level planning results on the NAVSIM dataset. \ddagger denotes that the model is initialized
 649 with weights pre-trained on the MetaAD dataset.

651 652 653 654 655 656	Method	Acc. (%)	Path (F1) \uparrow				Speed (F1) \uparrow		
			straight	left	right	keep	acc.	dec.	stop
	Qwen2VL (Wang et al., 2024a)	84.68	97.23	70.02	74.14	92.83	22.78	20.99	91.12
	AlphaDrive	<u>87.54</u>	<u>97.76</u>	<u>76.51</u>	<u>79.52</u>	<u>94.76</u>	<u>28.46</u>	<u>25.39</u>	<u>92.05</u>
	AlphaDrive \ddagger	92.44	98.67	83.53	82.21	95.12	45.27	53.94	95.31

657 Table 6: Abalation on different planning models and multimodal planning results on MetaAD dataset.

659 660 661 662 663 664 665	Method	# Samples	Acc. (%)	Path (F1) \uparrow				Speed (F1) \uparrow		
				straight	left	right	keep	acc.	dec.	stop
	ViT-L/14 \ddagger (Dosovitskiy et al., 2020)	1	36.77	78.19	52.48	57.27	72.26	25.41	43.50	74.15
	ViT-L/14 \ddagger (Dosovitskiy et al., 2020)	2	43.12	82.83	56.92	60.01	76.96	29.56	48.35	77.10
	Qwen2VL (Wang et al., 2024a)	1	55.84	82.68	80.31	70.04	75.97	34.92	55.55	72.64
	Qwen2VL (Wang et al., 2024a)	2	58.80	87.00	84.33	73.20	77.61	38.95	59.82	76.63
	AlphaDrive	1	<u>77.12</u>	<u>96.62</u>	<u>89.83</u>	<u>93.25</u>	<u>86.80</u>	<u>56.33</u>	<u>71.40</u>	<u>86.63</u>
	AlphaDrive	2	85.39	97.44	92.19	95.94	92.74	71.58	83.75	90.72

667 A APPENDIX

670 A.1 HIGH-LEVEL PLANNING RESULTS ON THE NAVSIM DATASET

671 We further evaluated the planning performance of AlphaDrive on the publicly available NAVSIM
 672 dataset (Dauner et al., 2024), as summarized in Tab. 5. The NAVSIM dataset was reformatted into
 673 visual question-answering data compatible with AlphaDrive. We compared the performance of three
 674 variants: (1) the original Qwen2VL-2B model trained via supervised fine-tuning (SFT) (first row),
 675 (2) the model trained using our proposed strategy (second row), and (3) the model first pretrained
 676 on the MetaAD dataset and subsequently fine-tuned on NAVSIM using our RL approach (third
 677 row). As shown, our training strategy leads to a substantial improvement in planning performance.
 678 Furthermore, pretraining on a larger-scale dataset enables the model to generalize effectively across
 679 diverse scenarios.

680 A.2 MULTIMODAL PLANNING CAPABILITY

682 We conducted an ablation study with multiple planning generation samples to assess the advantage of
 683 AlphaDrive over the SFT-trained model in terms of multimodal planning capabilities. A prediction is
 684 deemed correct if at least one of the generated actions matches the ground truth. As illustrated in
 685 Tab. 6, when sampling two candidates, AlphaDrive significantly outperforms Qwen2VL-2B trained
 686 with SFT, highlighting the effectiveness of our reinforcement learning strategy in improving the
 687 model’s ability to produce diverse and accurate planning actions.

689 A.3 COMPARISON WITH A SUPERVISED PLANNING CLASSIFIER

691 Since high-level planning can be formulated as a classification task over a finite set of actions,
 692 we further evaluated the performance of a simple vision classifier to emphasize the rationale and
 693 advantages of employing VLMs for planning. Specifically, we employ ViT-L/14 from CLIP (Radford
 694 et al., 2021) as the visual encoder, followed by two MLP classification heads to predict path and
 695 speed actions. To ensure consistency with AlphaDrive, we also provide state information such as
 696 navigation commands and ego speed to the classification heads. The classifier is trained using a
 697 weighted cross-entropy loss, which integrates action-specific weighting into the supervision signal
 698 similar to AlphaDrive’s GRPO reward design.

699 As shown in the first two rows of Tab. 6, this vision classifier exhibits poor planning performance, even
 700 underperforming the baseline Qwen2VL. These results highlight that, compared to pure vision models,
 701 VLMs equipped with commonsense knowledge and reasoning capabilities can more effectively
 702 improve high-level planning performance.

702
703
704
Table 7: End-to-end trajectory planning results on the MetaAD dataset.
705
706
707
708
709
710

Method	Type	Planning L2 (m) ↓					
		0.5s	1s	1.5s	2s	2.5s	3s
VADv2 (Chen et al., 2024a)	E2E	0.35	0.56	0.73	1.69	2.40	3.15
Qwen2VL (Wang et al., 2024a)	VLM	0.73	1.14	1.70	2.85	3.67	4.54
AlphaDrive-SFT	VLM+E2E	0.32	0.50	0.63	1.43	2.15	2.68
AlphaDrive	VLM+E2E	0.28	0.44	0.53	1.27	1.86	2.39

711
712
Table 8: Ablations on the training dataset size.
713
714
715
716
717
718
719
720
721
722

Train. Data	Train. Strategy	Acc. (%)	Path (F1) ↑			Speed (F1) ↑			BLEU-4	CIDEr	METEOR
			straight	left	right	acc.	dec.	stop			
20k	SFT	41.12	56.15	36.72	35.59	40.63	17.14	16.74	19.19	27.18	15.42
20k	RL	45.46	69.28	59.42	51.91	56.93	30.82	37.71	30.94	20.33	11.01
20k	SFT+RL	55.64	68.25	64.06	56.87	58.61	45.19	53.68	44.09	32.84	17.02
50k	SFT	53.02	73.74	62.45	65.43	70.07	33.83	38.94	53.96	34.48	26.83
50k	RL	59.33	77.69	68.55	73.82	77.05	40.72	45.20	57.06	22.37	16.81
50k	SFT+RL	70.83	82.30	78.05	82.17	84.80	47.27	58.29	64.67	32.30	30.38
110k	SFT	65.40	82.52	71.28	68.65	81.91	36.48	59.31	71.55	37.21	34.30
110k	RL	72.41	93.16	84.24	89.32	82.58	51.19	64.70	82.02	25.14	24.58
110k	SFT+RL	77.12	96.62	89.83	93.25	86.80	56.33	71.40	86.63	43.54	38.97

723
724
725
A.4 END-TO-END PLANNING RESULTS ON THE METAAD DATASET726
727
728
729
730
We also evaluate the effectiveness of AlphaDrive for end-to-end trajectory planning on the MetaAD dataset, as summarized in Tab. 7. The comparison models include the end-to-end model VADv2, the vision-language model Qwen2VL, and an SFT-trained baseline that shares the same architecture as AlphaDrive. We employ Qwen2VL as the VLM and VADv2 as the end-to-end module to ensure a fair comparison.731
732
733
734
735
The results indicate that directly using Qwen2VL for trajectory planning yields poor performance. Compared to the standalone end-to-end model, the SFT-trained baseline achieves moderate improvement by combining the VLM and end-to-end modules. Notably, AlphaDrive achieves the best planning performance among all evaluated methods, which demonstrates the effectiveness of AlphaDrive’s training strategy for driving planning.736
737
A.5 ABLATION STUDY ON TRAINING DATASET SIZE738
739
740
741
742
743
744
Fig. 1 illustrates the impact of different training data size and strategies on overall planning accuracy, while Tab. 8 provides a more detailed analysis. As observed, when the training data size decreases, SFT is more affected. With only 20k samples, the model trained with RL reaches a planning accuracy of 46.08%, which is significantly higher than that of the SFT-trained model. When using nearly half of the data, with 50k samples, AlphaDrive already achieves a planning accuracy of 70.83%, demonstrating the efficiency of our training strategy.745
746
A.6 MORE DATASET DETAILS747
748
749
750
751
The MetaAD dataset was collected by expert human drivers using a sensor suite that includes six surround-view cameras, one fisheye camera, and a LiDAR unit, while also recording navigation information and the ego odometry at each time step. The acquisition frequency is 2 Hz. After the raw data are collected, object bounding boxes and other annotations are generated using an offline, cloud-based labeling system.752
753
754
755
The final collection encompasses a range of weather conditions, including sunny, cloudy, and rainy days. It was captured in diverse environments such as urban areas, rural regions, and elevated highways, and provides a balanced distribution of various decision-making scenarios.